Targeted vaccination and the speed of SARS-CoV-2 adaptation

Sylvain Gandon[a,1,2] and Sébastien Lion[a,1]

[a]CEFE, CNRS, Univ Montpellier, EPHE, IRD, Montpellier, France

Edited by Eugene Koonin, National Center for Biotechnology Information, National Library of Medicine, NIH, Bethesda, MD; received June 22, 2021; accepted November 18, 2021

The limited supply of vaccines against severe acute respiratory syndrome coronavirus 2 (SARS-CoV-2) raises the question of targeted vaccination. Many countries have opted to vaccinate older and more sensitive hosts first to minimize the disease burden. However, what are the evolutionary consequences of targeted vaccination? We clarify the consequences of different vaccination strategies through the analysis of the speed of viral adaptation measured as the rate of change of the frequency of a vaccine-adapted variant. We show that such a variant is expected to spread faster if vaccination targets individuals who are likely to be involved in a higher number of contacts. We also discuss the pros and cons of dose-sparing strategies. Because delaying the second dose increases the proportion of the population vaccinated with a single dose, this strategy can both speed up the spread of the vaccine-adapted variant and reduce the cumulative number of deaths. Hence, strategies that are most effective at slowing viral adaptation may not always be epidemiologically optimal. A careful assessment of both the epidemiological and evolutionary consequences of alternative vaccination strategies is required to determine which individuals should be vaccinated first.

evolutionary epidemiology | vaccination | adaptation | COVID-19 | SARS-CoV-2

The development of effective vaccines against severe acute respiratory syndrome coronavirus 2 (SARS-CoV-2) raises hope regarding the possibility of eventually halting the ongoing pandemic. However, vaccine supply shortages have sparked a debate about the optimal distribution of vaccination among different categories of individuals. Typically, infections with SARS-CoV-2 are far more deadly in older individuals than in younger ones (1). Prioritizing vaccination for older classes may thus provide a direct benefit in terms of mortality (2, 3). Yet, younger individuals are usually more active, and consequently, they may contribute more to the spread of the epidemic. Prioritizing vaccination for younger and more active individuals may thus provide an indirect benefit through a reduction of the epidemic size (4, 5). Earlier studies have compared alternative ways to deploy vaccination in heterogeneous host populations and showed that recommendation varies with the choice of the quantity one is trying to minimize (e.g., the cumulative number of deaths, the remaining life expectancy, or the number of infections) (3, 6, 7). The recommendation also varies with the properties of the pathogen and the efficacy of the vaccine (3, 4, 8). For SARS-CoV-2, the increase in mortality with age is such that the direct benefit associated with vaccinating more vulnerable individuals tends to overwhelm the indirect benefits obtained from vaccinating more active individuals (2, 3, 9, 10). However, some studies challenge this view and identified specific conditions where vaccinating younger and more active classes could be optimal (5, 7, 11, 12). A similar debate emerges over the possibility to delay the second vaccination dose to maximize the number of partially vaccinated individuals. A quantitative exploration of alternative vaccination strategies can help provide useful recommendations: a two-dose strategy is recommended when the level of protection obtained after the first dose is low and/or when vaccine supply is large (13–16).

Vaccine-driven evolution, however, could erode the benefit of vaccination and alter the above recommendations which are based solely on the analysis of epidemiological dynamics. Given that hosts differ both in their sensitivity to the disease and in their contribution to transmission, who should we vaccinate first if we want to minimize the spread of vaccine-adapted variants? The effect of alternative vaccination strategies on the speed of pathogen adaptation remains unclear. Previous studies of adaptation to vaccines focused on long-term evolutionary outcomes (17, 18). These analyses are not entirely relevant for the ongoing pandemic because what we want to understand first is the short-term consequence of different vaccination strategies (19). A few studies have discussed the possibility of SARS-CoV-2 adaptation following different targeted vaccination strategies but did not explicitly account for evolutionary dynamics (12, 20). A recent simulation study explored the effect of a combination of vaccination and social distancing strategies on the probability of vaccine-driven adaptation (21). This model, however, did not study the impact of targeted vaccination strategies on the speed of adaptation.

Here we develop a theoretical framework based on the analysis of the deterministic dynamics of multiple variants after they successfully managed to reach a density at which they are no longer affected by the action of demographic stochasticity. We study the impact of different vaccination strategies on the rate of change of the frequency of a novel variant, which allows us to quantify the speed of virus adaptation to vaccines. Numerical

Significance

The ongoing pandemic of severe acute respiratory syndrome coronavirus 2 (SARS-CoV-2) raises an important question: who should we vaccinate first? Answering this question requires an analysis of both the short-term (epidemiological) and the long-term (evolutionary) consequences of targeted vaccination strategies. We analyze the speed of pathogen adaptation and the cumulative number of deaths in heterogeneous host populations to shed light on the effects of alternative vaccination strategies. This analysis shows that minimizing the speed of pathogen adaptation does not always minimize the number of deaths. This evaluation of both the epidemiological and evolutionary consequences of public health policies provides a practical tool to identify the best vaccination strategy.

Author contributions: S.G. and S.L. designed research, performed research, and wrote the paper.

The authors declare no competing interest.

This article is a PNAS Direct Submission.

This open access article is distributed under Creative Commons Attribution-NonCommercial-NoDerivatives License 4.0 (CC BY-NC-ND).

[1]S.G. and S.L. contributed equally to this work.

[2]To whom correspondence may be addressed. Email: sylvain.gandon@cefe.cnrs.fr.

This article contains supporting information online at https://www.pnas.org/lookup/suppl/doi:10.1073/pnas.2110666119/-/DCSupplemental.

Published January 14, 2022.

Downloaded from https://www.pnas.org by 194.57.116.220 on June 19, 2026 from IP address 194.57.116.220.

simulations tailored to the epidemiology of SARS-CoV-2 confirm the validity of our approximation of the strength of selection for vaccine-adapted variants.

Results

We are interested in tracking the frequency p_m of hosts infected by the vaccine-adapted variant among all the infected hosts. It is possible to show that under a broad range of conditions one can approximate the dynamics of the vaccine-adapted variant frequency as

$$\dot{p}_m \approx p_m(1-p_m)\mathcal{S}(t), \qquad [1]$$

where $\mathcal{S}(t)$ is the selection coefficient on the vaccine escape mutation. This selection coefficient measures the rate of change of the logit of the frequency of the vaccine-adapted variant [i.e., $\ln(p_m/(1-p_m))$] and provides a relevant measure for the speed at which the viral population is adapting (*Materials and Methods*).

Targeted vaccination strategies aim to preferentially vaccinate hosts according to specific epidemiological characteristics. For instance, we could target hosts that have more contacts or are more at risk for a severe disease. In our model, we therefore introduce some heterogeneity among hosts. As a result, from the point of view of the parasite, the quality of the host may differ among infected hosts, and this variation is likely to affect the dynamics of vaccine-adapted variants. To quantify host quality, we use the concept of reproductive value, a key concept in demography and evolutionary biology (22–24). Reproductive value measures how much a virus infecting a given class of hosts will contribute to the future of the viral population. Our general mathematical analysis allows us to take the difference in host quality into account when calculating the selection coefficient $\mathcal{S}(t)$ (*Materials and Methods*).

We use this approach to analyze the speed of adaptation during the ongoing pandemic of SARS-CoV-2 under different scenarios. We use an epidemiological model tailored to the biology of SARS-CoV-2 (*Materials and Methods*). However, it is important to keep in mind that due to simplifying assumptions and uncertainty about parameter values, our results cannot be translated directly into public health recommendations without further investigations (*Discussion*). Nonetheless, our theoretical framework gives clear foundations for future applied work and captures some of the most salient features of the COVID-19 pandemic. In particular, we introduce a time-varying parameter $c(t)$, which measures the intensity of nonpharmaceutical interventions (NPI). We assume that the epidemic is initially controlled by NPI, which yields successive epidemic waves before the deployment of vaccination at $t = 150$ d. We use this model to explore the effect of two different forms of heterogeneity on the speed of SARS-CoV-2 adaptation.

Heterogeneity in Contact Numbers and Vulnerability. In the first scenario we assume that hosts differ in their ability to mix and thus to transmit the disease. More specifically, following the model used by ref. 12, we assume that some hosts (L) have a low number of social interactions, while other hosts (H) have a higher number of contacts. These two types of hosts can be thought as corresponding to the older and younger halves of the population. The increased rate of social interactions among H hosts is captured by a parameter $\mathcal{M} \geq 1$. Susceptible hosts are initially naive (S^L and S^H), but they can become vaccinated ($\hat{S}^L$ and $\hat{S}^H$) at rates ν^L and ν^H, respectively. When vaccinated, hosts have a lower probability to become infected (r_σ measures the efficacy at blocking infection), and if they become infected, they have a lower probability to transmit the virus (r_τ measures the efficacy at blocking transmission) and to die from the infection (r_μ measures the efficacy at reducing mortality). Viral adaptation, however, can erode these benefits. We consider different viral strains characterized by an escape trait e which takes values between 0 (no escape) and 1 (full escape). The capacity of a variant to reduce the effect of the vaccine on transmissibility (infectivity) is captured by a function $E_\tau(e)$ for transmissibility (and $E_\sigma(e)$ for infectivity), which allows us to quantify the overall ability of the virus to escape the protective effects of the vaccine as $E(e) = E_\tau(e)E_\sigma(e)$. Note that the capacity of a variant to reduce mortality does not affect the strength of selection in our model (i.e., the duration of infection is affected neither by the variant nor by the vaccine).

In *Materials and Methods*, we derive a simple approximation for the strength of selection acting on the vaccine-adapted variant:

$$\mathcal{S}(t) = (1-c(t))\,\beta\,\Delta E\,\left(\hat{S}^L + \mathcal{M}^2\hat{S}^H\right), \qquad [2]$$

where ΔE refers to the change in vaccine escape ability caused by the mutation. This tells us that the intensity of selection depends on 1) the ability of the virus mutant to escape the protective effects of vaccine, 2) the densities of uninfected hosts (both L and H) who have been vaccinated, and 3) the relative number of contacts of each class of hosts. Note that the epidemiological impact of a higher contact rate ($\mathcal{M} > 1$) translates into a magnified selective impact ($\mathcal{M}^2$). Thus, if we have to choose between vaccinating L and H hosts, targeting H hosts is expected to select more strongly for the vaccine-adapted variant. Fig. 1*B* confirms that this approximation captures very well the temporal dynamics of the vaccine-adapted variant. In particular, the simulations confirm that targeted vaccination of the L hosts slows down the rate of adaptation of the virus.

Of course, the choice of the vaccination strategy should not be based solely on the reduction of the speed of adaptation to vaccines. Indeed, the best way to limit the spread of vaccine escape mutations would be to adopt the worst epidemiological strategy: avoiding the use of vaccines. Yet, we urgently need vaccines to save lives and halt the current pandemic. We can use our numerical simulations to study the consequences of distinct targeted vaccination strategies on the total number of cases and on mortality (*Materials and Methods*). Fig. 1*C* shows that targeting L hosts is expected to increase the number of cases because H hosts contribute more to the spread of the disease. Yet, Fig. 1*D* shows that targeting L hosts is expected to decrease the cumulative number of deaths after some time because L hosts (i.e., older individuals) are also associated with higher risks of dying from the infection. Hence, targeting L hosts makes sense both for epidemiological and evolutionary reasons.

We explored the robustness of the above results for a range of alternative scenarios. First, we note that as expected from our analytic approximation, the use of a transmission-blocking vaccine (instead of an infection-blocking vaccine) yields very similar outcomes (compare Fig. 1 and *SI Appendix*, Fig. S1). Second, we show in *SI Appendix*, Fig. S2 that evolution amplifies the increase in the cumulative number of deaths when H hosts are vaccinated compared to a scenario without viral adaptation. Indeed, the spread of a vaccine-adapted variant drives a large epidemic wave in vaccinated populations. This evolutionary effect is maximized for intermediate values of the speed of the vaccination rollout because when vaccine rollout is very fast, the vaccine-adapted variant is rapidly favored, whatever the targeted vaccination strategy (*SI Appendix*, Fig. S3). Finally, we note that maintaining social distancing for longer can substantially decrease the speed of adaptation (*SI Appendix*, Fig. S4).

Heterogeneity in the Number of Vaccination Doses. In our second scenario, we assume that the heterogeneity among hosts is determined by differential strength of immunity induced by distinct vaccination status. We distinguish between unvaccinated hosts (S), hosts partially vaccinated with one dose ($\hat{S}^{\mathrm{I}}$), and hosts "fully vaccinated" with two doses ($\hat{S}^{\mathrm{II}}$). Using the same approach as before, we obtain the following expression for the strength

Downloaded from https://www.pnas.org by 194.57.116.220 on June 19, 2026 from IP address 194.57.116.220.

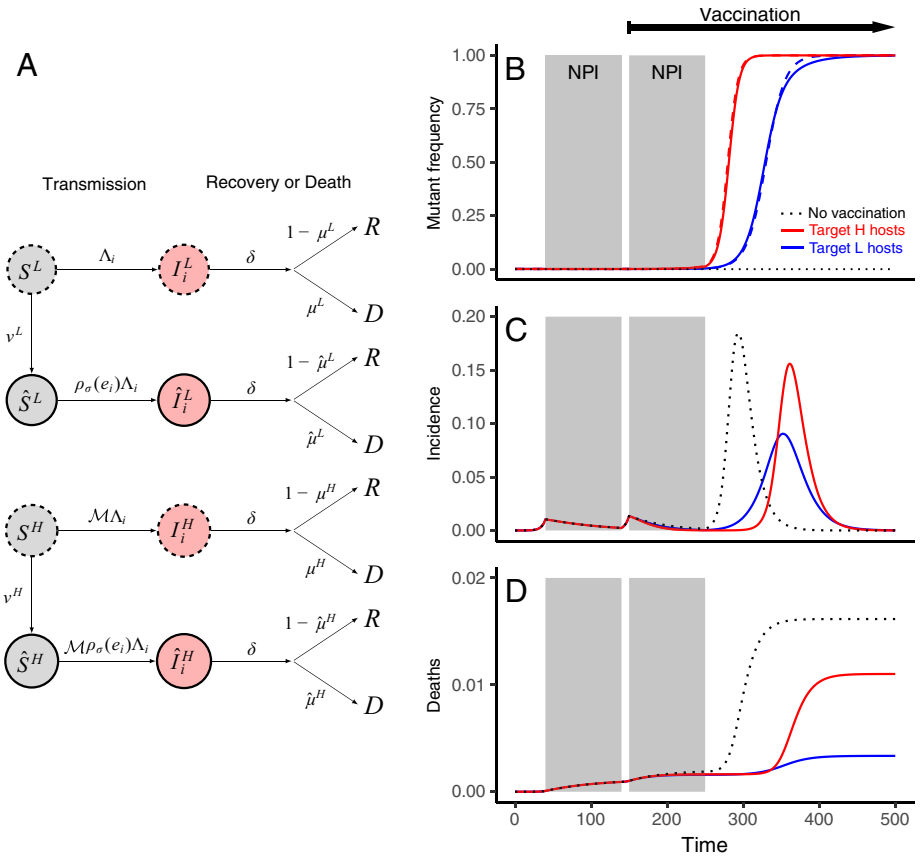

Fig. 1. Scenario 1: heterogeneity in contact numbers and vulnerability. (*A*) A graphical presentation of the epidemiological life cycle with *L* hosts who are more vulnerable to the disease and *H* hosts who have a higher number of contacts. Infected hosts are indicated with a light red shading, and vaccination is indicated with a bold circle border. The force of infection on naive hosts is noted $\Lambda_i = h_i + \hat{h}_i$ (see *Materials and Methods* and Table 1 for additional details on this model). (*B*) Dynamical change of the frequency p_m of the vaccine-adapted mutant for two distinct targeted vaccination strategies: 1) mostly *L* hosts are vaccinated (blue lines) and 2) mostly *H* hosts are vaccinated (red lines). The full lines indicate the exact numerical computation, and the dashed lines indicate the approximation obtained from Eq. **2**. The gray areas indicate the period where NPI were used to control the epidemic ($c(t) = 0.7$ with NPI). (*C*) Incidence of the epidemic (fraction of the total host population that is infected) in the absence of vaccination (dotted black line) or under the two alternative vaccination strategies used in *B* (blue and red lines). (*D*) Cumulative number of deaths (fraction of the total host population) in the absence of vaccination (dotted black line) or under the two alternative vaccination strategies used in *B* (blue and red lines).

of selection acting on the strength of selection on the vaccine-adapted variant:

$$\mathcal{S}(t) = (1 - c(t))\,\beta\,\left(\Delta E^{\mathrm{I}}\,\hat{S}^{\mathrm{I}} + \Delta E^{\mathrm{II}}\,\hat{S}^{\mathrm{II}}\right). \qquad [3]$$

Eq. **3** is very similar to Eq. **2**, but now we have to account for the fact that the escape mutation has different effects in each class. Hence, the influences of an increase in the densities of hosts vaccinated by a single or two doses of vaccines are weighted by ΔE^{I} and ΔE^{II}, respectively. A single vaccine dose is likely to induce a lower protection against the virus (i.e., $E^{\mathrm{I}} > E^{\mathrm{II}}$), but this does not necessarily imply that $\Delta E^{\mathrm{I}} > \Delta E^{\mathrm{II}}$. In fact, we can show that if the vaccine is acting on a single step of the virus' life cycle (e.g., only blocking infection), we expect $\Delta E^{\mathrm{II}} > \Delta E^{\mathrm{I}}$. Delaying the acquisition of the second dose will have two effects: 1) a lower density $\hat{S}^{\mathrm{II}}$ of fully vaccinated hosts decreases the more intense selection imposed by these hosts but 2) delaying the second dose allows for more hosts to be vaccinated, and the increase in $\hat{S}^{\mathrm{I}}$ may result in stronger selection for the vaccine-adapted variants. We show in Fig. 2*B* that this second effect can be more important than the first one, and delaying the second dose can result in faster adaptation. However, Fig. 2*D* shows that delaying the second dose may reduce the cumulative number of deaths because a larger fraction of the population would benefit from the protection of the vaccine (but higher rates of vaccination rollout can reverse this effect on mortality; *SI Appendix*, Figs. S5 and S6). Hence, in contrast to the previous scenario, the strategy that maximizes the speed of adaptation may result in a lower mortality. The contrast between our two scenarios illustrates the necessity to quantify both the epidemiological and the evolutionary consequences of different targeted vaccination strategies to identify the optimal way to distribute vaccines.

Discussion

The speed of the spread of SARS-CoV-2 variants has baffled the scientific community (25, 26). Despite a relatively small mutation rate (27, 28), SARS-CoV-2 has the ability to produce mutations with variable phenotypic effects that fuel the adaptation to human populations. The growing concern regarding the ability of the virus to escape host immunity calls for tools allowing us to anticipate the speed of the spread of vaccine escape mutants. We show here that heterogeneity in the behavior (scenario 1) and/or immune status (scenario 2) of the human host can induce variation in the strength of selection for vaccine escape mutations in the virus population. We contend that it is important to quantify this variation because it could be used to carry out targeted vaccination strategies that, for a given vaccination coverage, could limit the speed of adaptation of the virus.

We show that targeted vaccination on older hosts which are associated with lower number of contacts but higher risks of

Downloaded from https://www.pnas.org by 194.57.116.220 on June 19, 2026 from IP address 194.57.116.220.

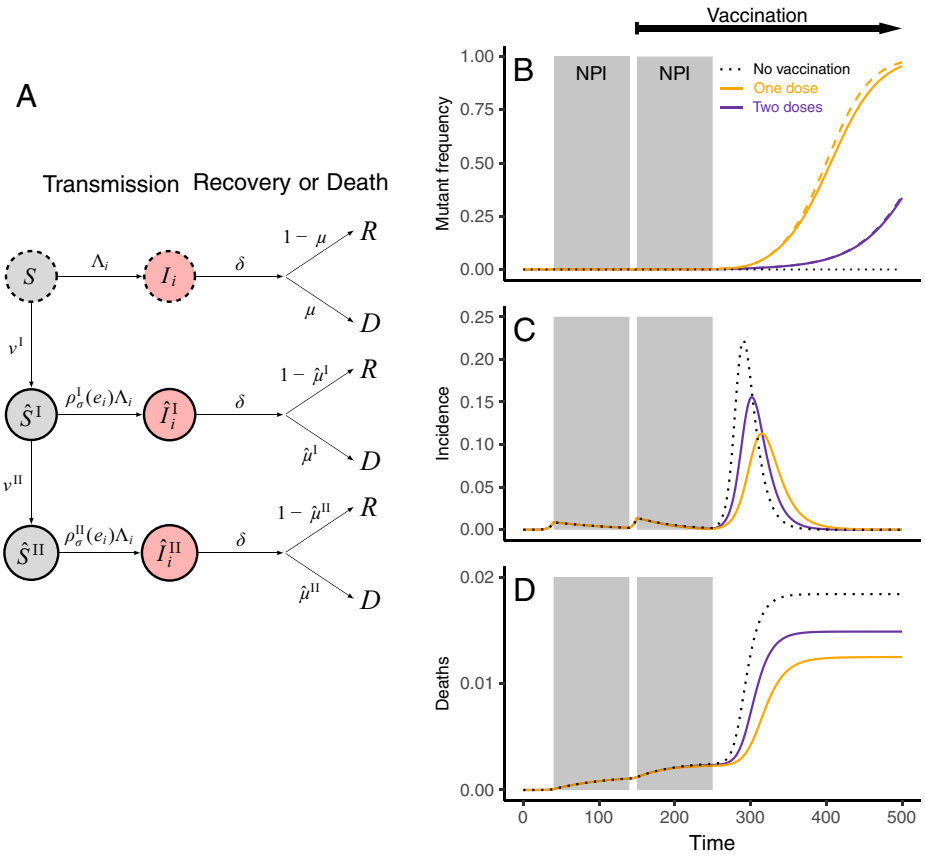

Fig. 2. Scenario 2: heterogeneity in the number of vaccination doses. (*A*) A graphical presentation of the epidemiological life cycle where the superscripts I and II refer to the first and second doses of vaccine. Infected hosts are indicated with a light red shading, and vaccination is indicated with a bold circle border. The force of infection on naive hosts is noted $\Lambda_i = h_i + \hat{h}_i$ (see *Materials and Methods* and Table 2 for additional details on this model). (*B*) Dynamical change of the frequency p_m of the vaccine-adapted mutant for two distinct targeted vaccination strategies: 1) vaccinated hosts receive two doses sequentially (purple lines) and 2) a single dose is used for each host (orange lines). The full lines indicate the exact numerical computation, and the dashed lines indicate the approximation obtained from Eq. **3**. The gray areas indicate the period where NPI were used to control the epidemic ($c(t) = 0.7$ with NPI). (*C*) Incidence of the epidemic (fraction of the total host population that is infected) in the absence of vaccination (dotted black line) or under the two alternative vaccination strategies used in *B* (purple and orange lines). (*D*) Cumulative number of deaths (fraction of the total host population) in the absence of vaccination (dotted black line) or under the two alternative vaccination strategies used in *B* (purple and orange lines).

mortality may be a good strategy to reduce both the spread of the vaccine escape variant and the cumulative number of deaths. Ref. 12 used a different approach to identify vaccination strategies that could reduce what they call "vaccine escape pressure," a quantity proportional to the density of infected hosts who are vaccinated. In contrast, we show that the strength of selection on the vaccine-adapted mutant is proportional to the density of susceptible hosts who are vaccinated. Their analysis relies on the assumption that the incidence of the infection remains small (i.e., no depletion of susceptible hosts), and they do not track explicitly the rate of spread of a vaccine-adapted variant. They conclude that vaccinating most of the vulnerable hosts and few of the mixers could be the most risky for vaccine escape. Yet, it is difficult to evaluate how the vaccine escape pressure criteria used in ref. 12 may affect the speed of viral adaptation. A high incidence among vaccinated hosts may speed up viral adaptation because a vaccine-adapted variant generated by mutation is more likely to escape extinction in a vaccinated host. However, a quantification of this effect would require an explicit description of the interplay between within-host selection and demographic stochasticity. In other words, their model focuses on the process that limits the emergence of vaccine-adapted variants, while our analysis focuses on the strength of selection after emergence. It would thus be particularly interesting to explore the robustness of our results with a model that would account for the effects of demographic stochasticity and within-host selection on the emergence of new variants.

We also discuss the effect of delaying the second dose of the vaccine on viral adaptation and on mortality. In a recent model, ref. 29 found that imperfect immunity induced by a single dose may lead to stronger within-host selection for vaccine escape variants. This is the same argument used by ref. 12, where the infection of imperfectly immunized hosts may speed up viral adaptation. However, as discussed above, this effect relies on the interplay between demographic stochasticity and within-host selection. In contrast, we focus on between-host selection and ask whether vaccine-adapted variants can increase in frequency at the population level. We contend that once vaccine-adapted variants reach a significant fraction of the population, the fate of those mutations will be driven by between-host selection. Our analysis clarifies the balance between the effects of mutations in different types of hosts (i.e., the relative magnitudes of ΔE^{I} and ΔE^{II}) and the quantity of the different types of hosts (i.e., the relative densities of hosts with one or two doses of the vaccine). We show that a higher speed of adaptation may be the price to pay for a reduced number of deaths (Fig. 2*B*). Indeed, delaying the second dose allows for protecting (albeit partially) a larger fraction of the population (see ref. 15 for an exploration of this effect). This positive effect can outweigh the negative consequences of an erosion of vaccine efficacy due to viral adaptation.

Downloaded from https://www.pnas.org by 194.57.116.220 on June 19, 2026 from IP address 194.57.116.220.

Interestingly, we found that combining vaccination and NPI can delay the rise of vaccine-adapted variants (*SI Appendix*, Figs. S4 and S7). Our analysis clarifies the origin of the positive effect of NPI discussed in previous studies (21, 30). In our deterministic model, this effect emerges from the reduction in the strength of between-host selection due to lower opportunities of transmission (i.e., see the effect of larger values of $c(t)$ in Eqs. **2** and **3**).

Vaccination is urgently needed to control the SARS-CoV-2 pandemic, but the limited supply of vaccines is raising major ethical and practical issues. Public health policies need to strike a balance between social, ethical, and short-term epidemiological considerations. Our work illustrates that the long-term evolutionary consequences of specific vaccination strategies also need to be considered and evaluated using quantitative models. Indeed, viral adaptation could erode the efficacy of vaccines, and targeted vaccination may provide a way to delay this adaptation. Yet, as illustrated with the second scenario, a strategy that minimizes the cumulative number of deaths may not necessarily minimize the speed of adaptation. Hence, as for any therapeutic interventions that may result in the evolution of pathogen resistance, the identification of an optimal vaccination strategy that reduces the death toll of the pandemic requires specific models accounting for both the epidemiology and the evolution of the virus (31–33). Because our model relies on several simplifying assumptions and because our knowledge of the biology of SARS-Cov-2 and of several key parameter values (e.g., vaccine efficacy, virulence, and contact rates) remains imperfect, our model cannot be used directly to make quantitative public health recommendations. Nonetheless, our framework lays a clear conceptual foundation to analyze the consequences of targeted vaccination strategies. In order to make more precise applied predictions, it would be interesting to investigate how other realistic factors (such as age structure, difference in transmissibility among host classes, or alternative vaccination schedules) may affect our results. Furthermore, the present work could be readily extended to combine the two forms of heterogeneities in the same model to allow for alternative ways to distribute the vaccines (e.g., two doses for L individuals and one dose for H individuals). It would also be possible to use the same framework to account for other factors that have been shown to affect the outcome of vaccination strategy like assortative mixing (4) and compensatory behavior after vaccination (34). In all these scenarios, our framework could be used to identify which strategy manages to strike the right balance between the epidemiological and the evolutionary consequences of targeted vaccination strategies.

Materials and Methods

General Approach. We first give a general overview of the method used to calculate the selection coefficient in structured host populations. The dynamics of hosts infected by pathogen strain i can be captured by a matrix $\mathbf{R}_i$ collecting the transition rates between host classes. Assuming that mutations have small phenotypic effects (i.e., $e_m = e_w + \varepsilon$), we can write the change in frequency of the mutant strain as

$$\frac{dp_m}{dt} = \varepsilon p_m(1-p_m)\,\mathbf{v}^\top \frac{d\mathbf{R}_m}{de_m}\mathbf{f} + O(\varepsilon^2), \qquad [4]$$

where $\mathbf{v}^\top$ is the vector of reproductive values and $\mathbf{f}$ is the vector of class frequencies. These vectors are conormalized such that $\mathbf{v}^\top\mathbf{f} = 1$ and satisfy the following dynamical equations:

$$\frac{d\mathbf{f}}{dt} = \mathbf{R}_w\mathbf{f} - \lambda(t)\mathbf{f}, \qquad [5]$$

$$\frac{d\mathbf{v}^\top}{dt} = -\mathbf{v}^\top\mathbf{R}_w + \lambda(t)\mathbf{v}^\top, \qquad [6]$$

where $\mathbf{R}_w$ is the transition matrix for the wild-type strain and $\lambda(t)$ is the per-capita growth rate of the resident population at time t (see refs. 24, 35 for a more detailed description). The $d\mathbf{R}_m/de_m$ term in Eq. **6** refers to the differentiation of each element of the transition matrix $\mathbf{R}_m$ with respect to the effect of the mutant. For small ε, the mutant frequency p_m changes slowly compared to the ecological variables $\mathbf{f}$ and $\mathbf{v}$, and we can use a quasi-equilibrium approximations obtained by setting the right-hand sides of Eqs. **5** and **6** to zero. This allows us to obtain analytical expressions for the class frequencies and reproductive values and thus to calculate the selection coefficient for a specific life cycle (scenario 1 vs. scenario 2). Note that although the weak selection assumption (small ε) is driving the separation of time scale, the approximation remains good when selection is strong as discussed in the two scenarios below and shown in Figs. 1 and 2. The Mathematica notebooks used to generate Figs. 1 and 2 and *SI Appendix*, Figs. S1–S7 are accessible from the following data repository, https://doi.org/10.5281/zenodo.5803062.

Scenario 1: Should We Preferentially Vaccinate Individuals with More Contacts? We assume that susceptible hosts in class k (where $k = L$ or H) are vaccinated at rate ν^k representing the speed of vaccination rollout in that host class. We note $\mathcal{M} > 1$ as the relative number of contacts of H hosts compared to L hosts and ρ_τ (ρ_σ) as the relative transmissibility (susceptibility) of vaccinated hosts compared to naive hosts of the same class. Both ρ_τ and ρ_σ are functions of the vaccine escape trait. With these assumptions, the force of infection of a pathogen strain i due to naive infected hosts is $h_i = \beta_i^L I_i^L + \mathcal{M}\beta_i^H I_i^H$, and $\hat{h}_i = \rho_\tau(e_i)(\beta_i^L \hat{I}_i^L + \mathcal{M}\beta_i^H \hat{I}_i^H)$ for vaccinated infected hosts. Note that vaccinated hosts are indicated by a "hat" (denoting protection). Hosts in class k infected by pathogen strain i eventually leave the class at rate δ_i^k ($\hat{\delta}_i^k$ for vaccinated hosts) and can either recover or die. We assume that the probability μ_i^k ($\hat{\mu}_i^k$) of dying after leaving the class I_i^k ($\hat{I}_i^k$) may depend on the host class k and pathogen strain i. We track the cumulative number of deaths D. This quantity can be used to compare the efficacy of different vaccination strategies. Note that the probabilities μ_i^k and $\hat{\mu}_i^k$ have no impact on evolutionary dynamics because these events occur when the host is assumed to be no longer infectious, and consequently, they do not affect pathogen fitness.

This yields the following dynamical system (see also Fig. 1*A*):

$$\begin{aligned}
\dot{S}^L &= -\nu^L S^L - (h_i + \hat{h}_i)S^L \\
\dot{\hat{S}}^L &= \nu^L S^L - (h_i + \hat{h}_i)\rho_\sigma(e_i)\hat{S}^L \\
\dot{S}^H &= -\nu^H S^H - \mathcal{M}(h_i + \hat{h}_i)S^H \\
\dot{\hat{S}}^H &= \nu^H S^H - \mathcal{M}(h_i + \hat{h}_i)\rho_\sigma(e_i)\hat{S}^H \\
\dot{I}_i^L &= (h_i + \hat{h}_i)S^L - \delta_i^L I_i^L \\
\dot{\hat{I}}_i^L &= (h_i + \hat{h}_i)\rho_\sigma(e_i)\hat{S}^L - \hat{\delta}_i^L \hat{I}_i^L \\
\dot{I}_i^H &= \mathcal{M}(h_i + \hat{h}_i)S^H - \delta_i^H I_i^H \\
\dot{\hat{I}}_i^H &= \mathcal{M}(h_i + \hat{h}_i)\rho_\sigma(e_i)\hat{S}_i^H - \hat{\delta}_i^H \hat{I}_i^H \\
\dot{D} &= \sum_i \left(\mu_i^L \delta_i^L I_i^L + \hat{\mu}_i^L \hat{\delta}_i^L \hat{I}_i^L + \mu_i^H \delta_i^H I_i^H + \hat{\mu}_i^H \hat{\delta}_i^H \hat{I}_i^H\right).
\end{aligned} \qquad [7]$$

We analyze this general model under two simplifying but reasonable assumptions.

1. We assume that the pathogen strains only differ through their effect on the parameters ρ_τ and ρ_σ (that is, we only look at vaccine escape mutations, not mutations that can also affect transmissibility or virulence).
2. We assume that host classes L and H only differ through their number of contacts, so that $\delta_i^L = \hat{\delta}_i^L = \delta_i^H = \hat{\delta}_i^H = \delta$ and $\beta_i^L = \beta_i^H = \beta(1 - c(t))$, where β is the baseline transmissibility and $1 - c(t)$ captures the effect of NPI aimed at controlling the epidemic by reducing transmission. The parameter $c(t)$ varies between 0 and 1 and quantifies the intensity of the control, which may vary over time as observed during the COVID-19 pandemic.

The latter assumption implies that the duration of infection is the same in all classes, but the effect of vaccination on the mortality of the different classes of hosts can be captured through the probabilities μ^L, $\hat{\mu}^L$, μ^H, and $\hat{\mu}^H$ (again, note that there is no influence of the pathogen genotype on disease outcome). For instance, in our simulations, we assume that L hosts tend to have fewer contacts but a higher mortality risk, while H hosts have more contacts but a lower mortality risk. This may reflect the observed differences between age classes.

The transition matrix $\mathbf{R}_i$ is the 4×4 matrix of per-capita transition rates of the pathogen between the four different types of hosts, given by Eq. **8**.

Downloaded from https://www.pnas.org by 194.57.116.220 on June 19, 2026 from IP address 194.57.116.220.

$$\mathbf{R}_i = \begin{pmatrix} \beta^L S^L - \delta^L & \beta^L \rho_\tau(\mathbf{e}_i) S^L \\ \beta^L \rho_\sigma(\mathbf{e}_i) \hat{S}^L & \beta^L \rho_\tau(\mathbf{e}_i) \rho_\sigma(\mathbf{e}_i) \hat{S}^L - \hat{\delta}^L \\ \mathcal{M}\beta^L S^H & \mathcal{M}\beta^L \rho_\tau(\mathbf{e}_i) S^H \\ \mathcal{M}\beta^L \rho_\sigma(\mathbf{e}_i) \hat{S}^H & \mathcal{M}\beta^L \rho_\tau(\mathbf{e}_i) \rho_\sigma(\mathbf{e}_i) \hat{S}^H \\ \mathcal{M}\beta^H S^L & \mathcal{M}\beta^H \rho_\tau(\mathbf{e}_i) S^L \\ \mathcal{M}\beta^H \rho_\sigma(\mathbf{e}_i) \hat{S}_I & \mathcal{M}\beta^H \rho_\tau(\mathbf{e}_i) \rho_\sigma(\mathbf{e}_i) \hat{S}^L \\ \mathcal{M}^2 \beta^H S^H - \delta^H & \mathcal{M}^2 \beta^H \rho_\tau(\mathbf{e}_i) S^H \\ \mathcal{M}^2 \beta^H \rho_\sigma(\mathbf{e}_i) \hat{S}^H & \mathcal{M}^2 \beta^H \rho_\tau(\mathbf{e}_i) \rho_\sigma(\mathbf{e}_i) \hat{S}^H - \hat{\delta}^H \end{pmatrix}. \quad [8]$$

We are interested in the dynamics of the frequency of the vaccine escape mutant, which is

$$p_m = \frac{I_m^L + I_m^H + \hat{I}_m^L + \hat{I}_m^H}{\sum_i \left(I_i^L + I_i^H + \hat{I}_i^L + \hat{I}_i^H \right)}. \quad [9]$$

The dynamics of p_m can be calculated by plugging the expressions of $\mathbf{R}_w$ and $\mathbf{R}_m$ into Eqs. **4–6**. After some rearrangements, we obtain

$$\begin{aligned} \mathcal{S}(t) = & \frac{\mathrm{d}\rho_\sigma}{\mathrm{d}e_m} h_w \left(\hat{v}^L \hat{S}^L + \mathcal{M} \hat{v}^H \hat{S}^H \right) \\ & + \frac{\mathrm{d}\rho_\tau}{\mathrm{d}e_m} \hat{h}_w \left(v^L S^L + \rho_\sigma(\mathbf{e}_w) \hat{v}^L \hat{S}^L + \mathcal{M} v^H S^H \right. \\ & \left. + \mathcal{M} \rho_\sigma(\mathbf{e}_w) \hat{v}^H \hat{S}^H \right), \end{aligned} \quad [10]$$

where the vector $\mathbf{v}^\mathsf{T} = \begin{pmatrix} v^L & \hat{v}^L & v^H & \hat{v}^H \end{pmatrix}$ collects the reproductive values of an individual resident pathogen in classes I^L, $\hat{I}^L$, I^H, and $\hat{I}^H$, respectively. Note that this result only depends on assumption 1 above.

It is possible to simplify the expression of the selection coefficient by treating the reproductive values as fast variables. In particular, using our assumption 2, this leads to the following quasi-equilibrium approximations:

$$\frac{\hat{v}^L}{v^L} = \frac{\hat{v}^H}{v^H} = \rho_\tau(\mathbf{e}_w), \qquad \frac{v^H}{v^L} = \mathcal{M}, \qquad \frac{\hat{v}^H}{v^L} = \mathcal{M} \rho_\tau(\mathbf{e}_w). \quad [11]$$

Similarly, we have the following quasi-equilibrium approximations for the class frequencies, which give the fraction of infected individuals in a given class:

$$\frac{\hat{f}^L}{f^L} = \rho_\sigma(\mathbf{e}_w) \frac{\hat{S}^L}{S^L}, \qquad \frac{f^H}{f^L} = \mathcal{M} \frac{S^H}{S^L}, \qquad \frac{\hat{f}^H}{f^L} = \mathcal{M} \rho_\sigma(\mathbf{e}_w) \frac{\hat{S}^H}{S^L}. \quad [12]$$

Together with the normalization condition $v^L f^L + \hat{v}^L \hat{f}^L + v^H f^H + \hat{v}^H \hat{f}^H = 1$, we can use these relationships to obtain

$$\mathcal{S}(t) = \varepsilon \beta (1 - c(t)) \left(\hat{S}^L + \mathcal{M}^2 \hat{S}^H \right) \left. \frac{\mathrm{d}(\rho_\sigma \rho_\tau)}{\mathrm{d}e_m} \right|_{e_m = e_w}. \quad [13]$$

To recover Eq. **2**, we use the notations $E_\tau = \rho_\tau$, $E_\sigma = \rho_\sigma$, $E = E_\tau E_\sigma$, and

$$\Delta E = \varepsilon \left. \frac{\mathrm{d}E}{\mathrm{d}e_m} \right|_{e_m = e_w},$$

which is the first-order approximation of the difference $E(\mathbf{e}_m) - E(\mathbf{e}_w)$.

Numerical simulations. In our applications, we use a linear model of vaccine escape:

$$\rho_\tau(\mathbf{e}_i) = 1 - r_\tau(1 - \mathbf{e}_i), \quad [14]$$

$$\rho_\sigma(\mathbf{e}_i) = 1 - r_\sigma(1 - \mathbf{e}_i), \quad [15]$$

where r_τ and r_σ give the vaccine efficacy in the absence of vaccine escape mutation (i.e., $\mathbf{e}_i = 0$). When $\mathbf{e}_i = 1$ (full vaccine escape), the vaccine offers no reduction in transmissibility and susceptibility ($\rho_\sigma = \rho_\tau = 1$). As explained above, we assume that L hosts have a higher risk of mortality due to the disease and note $\mathcal{D}$ as the relative increase in mortality of L hosts vs. H hosts, μ as the baseline mortality probability, and $\rho_\mu = 1 - r_\mu$ as the reduction in mortality due to the vaccine (which we assume independent of host classes and of pathogen genotype). We thus have

$$\begin{aligned} \mu^L &= \mathcal{D}\,\mu \\ \hat{\mu}^L &= \rho_\mu\,\mathcal{D}\,\mu \\ \mu^H &= \mu \\ \hat{\mu}^H &= \rho_\mu\,\mu, \end{aligned}$$

with $\mathcal{D} > 1$ and $0 < \rho_\mu < 1$.

Initial conditions used in Fig. 1 *B–D* are as follows: $S^L(0) = S^H(0) = 1/2$, $\hat{S}^L = \hat{S}^H = 0$, $I^L(0) = I^H(0) = 10^{-6}$, $\hat{I}^L(0) = \hat{I}^H(0) = 10^{-6}$, $D(0) = 0$, and $p_m(0) = 10^{-3}$. The intensity of NPI varies with time ($c(t) = 0.7$ when $t \in [40, 140]$ and $t \in [150, 250]$, $c(t) = 0$ otherwise). Vaccination starts at $t = 150$, and the other parameters used in Fig. 1 *B–D* are listed in Table 1.

Table 1. Main parameters and default values used in scenario 1

Parameters	Symbol	Values
Virus parameters		
Basic reproduction ratio	R_0	3
Transmission	β	0.12 d^{-1}
Recovery rate	δ	0.1 d^{-1}
Baseline probability of death	μ	0.001
Increased contact rate of H hosts	$\mathcal{M}$	2
Increased mortality of L hosts	$\mathcal{D}$	20
Infectivity of wild type on vaccinated hosts	$\mathbf{e}_w$	0
Infectivity of mutant type on vaccinated hosts	$\mathbf{e}_m$	0.8
Vaccine parameters		
Vaccination rate of L hosts	ν^L	0.02 d^{-1} (blue), 0.002 d^{-1} (red)
Vaccination rate of H hosts	ν^H	0.002 d^{-1} (blue), 0.02 d^{-1} (red)
Efficacy at blocking infection	r_σ	0.9
Efficacy at blocking transmission	r_τ	0
Efficacy at reducing mortality	r_μ	0.9

Scenario 2: Should We Delay the Second Dose? For our second scenario, we consider three classes of susceptible hosts: unvaccinated (S), vaccinated with one dose (S^I), and vaccinated with two doses (S^II). Unvaccinated susceptible hosts can be given a first dose of vaccine at rate ν^I. Susceptible hosts that have received one dose can be given a second dose at rate ν^II. With one dose, the relative transmissibility (susceptibility) of vaccinated hosts with respect to pathogen strain $\mathbf{e}_i$ is $\rho_\tau^\mathrm{I}(\mathbf{e}_i)$ ($\rho_\sigma^\mathrm{I}(\mathbf{e}_i)$). With two doses, we use the notation $\rho_\tau^\mathrm{II}(\mathbf{e}_i)$ and $\rho_\sigma^\mathrm{II}(\mathbf{e}_i)$. Apart from these assumptions, the life cycle is similar to the one used for scenario 1, and we have the following dynamics (see also Fig. 2*A*):

$$\begin{aligned} \dot{S} &= -\nu^\mathrm{I} S - (h_i + \hat{h}_i) S \\ \dot{S}^\mathrm{I} &= \nu^\mathrm{I} S - \nu^\mathrm{II} \hat{S}^\mathrm{I} - (h_i + \hat{h}_i) \rho_\sigma^\mathrm{I}(\mathbf{e}_i) \hat{S}^\mathrm{I} \\ \dot{S}^\mathrm{II} &= \nu^\mathrm{II} \hat{S}^\mathrm{I} - (h_i + \hat{h}_i) \rho_\sigma^\mathrm{II}(\mathbf{e}_i) \hat{S}^\mathrm{II} \\ \dot{I}_i &= (h_i + \hat{h}_i) S - \delta_i I_i \\ \dot{\hat{I}}_i^\mathrm{I} &= (h_i + \hat{h}_i) \rho_\sigma^\mathrm{I}(\mathbf{e}_i) \hat{S}^\mathrm{I} - \hat{\delta}_i^\mathrm{I} \hat{I}_i^\mathrm{I} \\ \dot{\hat{I}}_i^\mathrm{II} &= (h_i + \hat{h}_i) \rho_\sigma^\mathrm{II}(\mathbf{e}_i) \hat{S}^\mathrm{II} - \hat{\delta}_i^\mathrm{II} \hat{I}_i^\mathrm{II} \\ \dot{D} &= \sum_i \left(c_i \delta_i I_i + \hat{c}_i^\mathrm{I} \hat{\delta}_i^\mathrm{I} \hat{I}_i^\mathrm{I} + \hat{c}_i^\mathrm{II} \hat{\delta}_i^\mathrm{II} \hat{I}_i^\mathrm{II} \right), \end{aligned} \quad [16]$$

where the forces of infection by virus strain i are $h_i = \beta_i I_i$ and $\hat{h}_i = \rho_\tau^\mathrm{I}(\mathbf{e}_i) \beta_i^\mathrm{I} \hat{I}_i^\mathrm{I} + \rho_\tau^\mathrm{II}(\mathbf{e}_i) \beta_i^\mathrm{II} \hat{I}_i^\mathrm{II}$. For simplicity, we will also assume, as in scenario 1, that $\beta_i = \beta_i^\mathrm{I} = \beta_i^\mathrm{II} = \beta(1 - c(t))$ and $\delta_i = \hat{\delta}_i^\mathrm{I} = \hat{\delta}_i^\mathrm{II} = \delta$, so that 1) hosts only differ through the parameters ρ_τ and ρ_σ and 2) the viral strains only differ through the parameters ρ_τ and ρ_σ. We also assume that $\mu_i = \mu$, $\hat{\mu}_i^\mathrm{I} = \hat{\mu}^\mathrm{I}$, and $\hat{\mu}_i^\mathrm{II} = \hat{\mu}^\mathrm{II}$ to account for potential differences between mortality rates between different classes of hosts (but no influence of the pathogen genotype).

With these assumptions, the matrix $\mathbf{R}_i$ is

$$\mathbf{R}_i = \beta(1 - c(t)) \begin{pmatrix} S & \rho_\tau^\mathrm{I}(\mathbf{e}_i) S & \rho_\tau^\mathrm{II}(\mathbf{e}_i) S \\ \rho_\sigma^\mathrm{I}(\mathbf{e}_i) \hat{S}^\mathrm{I} & \rho_\tau^\mathrm{I}(\mathbf{e}_i) \rho_\sigma^\mathrm{I}(\mathbf{e}_i) \hat{S}^\mathrm{I} & \rho_\tau^\mathrm{II}(\mathbf{e}_i) \rho_\sigma^\mathrm{I}(\mathbf{e}_i) \hat{S}^\mathrm{I} \\ \rho_\sigma^\mathrm{II}(\mathbf{e}_i) \hat{S}^\mathrm{II} & \rho_\tau^\mathrm{I}(\mathbf{e}_i) \rho_\sigma^\mathrm{II}(\mathbf{e}_i) \hat{S}^\mathrm{II} & \rho_\tau^\mathrm{II}(\mathbf{e}_i) \rho_\sigma^\mathrm{II}(\mathbf{e}_i) \hat{S}^\mathrm{II} \end{pmatrix} - \delta \mathbf{J}, \quad [17]$$

where $\mathbf{J}$ is the 3×3 identity matrix, and the quasi-equilibrium relationships for class frequencies and reproductive values are

$$\frac{v^\mathrm{I}}{v^0} = \rho_\tau^\mathrm{I}(\mathbf{e}_w), \qquad \frac{v^\mathrm{II}}{v^0} = \rho_\tau^\mathrm{II}(\mathbf{e}_w)$$

and

$$\frac{f^\mathrm{I}}{f^0} = \rho_\sigma^\mathrm{I}(\mathbf{e}_w) \frac{\hat{S}^\mathrm{I}}{S}, \qquad \frac{f^\mathrm{II}}{f^0} = \rho_\sigma^\mathrm{II}(\mathbf{e}_w) \frac{\hat{S}^\mathrm{II}}{S},$$

where $\mathbf{v} = \begin{pmatrix} v^0 & v^\mathrm{I} & v^\mathrm{II} \end{pmatrix}$ and $\mathbf{f} = \begin{pmatrix} f^0 & f^\mathrm{I} & f^\mathrm{II} \end{pmatrix}$. Together with the normalization condition $v^0 f^0 + v^\mathrm{I} f^\mathrm{I} + v^\mathrm{II} f^\mathrm{II} = 1$, these relationships allow us to rearrange Eq. **4** to obtain

Downloaded from https://www.pnas.org by 194.57.116.220 on June 19, 2026 from IP address 194.57.116.220.

Table 2. Main parameters and default values used in scenario 2

Parameters	Symbol	Values
Virus parameters		
Basic reproduction ratio	R_0	3
Transmission	β	0.3 d^{-1}
Recovery rate	δ	0.1 d^{-1}
Baseline probability of death	μ	0.01
Infectivity of wild type on vaccinated hosts	e_w	0
Infectivity of mutant type on vaccinated hosts	e_m	0.8
Vaccine parameters		
Vaccination rate for 1st dose	ν^{I}	0.002 d^{-1} (purple), 0.004 d^{-1} (orange)
Vaccination rate for 2nd dose	ν^{II}	0.002 d^{-1} (purple), 0.0002 d^{-1} (orange)
Efficacy at blocking infection (1st and 2nd dose)	r_σ^{I}, r_σ^{II}	0.6 (1st dose) and 0.9 (2nd dose)
Efficacy at blocking transmission (1st and 2nd dose)	r_τ^{I}, r_τ^{II}	0 (1st dose) and 0 (2nd dose)
Efficacy at reducing mortality (1st and 2nd dose)	r_μ^{I}, r_μ^{II}	0.5 (1st dose) and 0.95 (2nd dose)

$$\mathcal{S}(t) = \varepsilon\beta(1-c(t))\left(\hat{S}^{\mathrm{I}}\left.\frac{\mathrm{d}(\rho_\sigma^{\mathrm{I}}\rho_\tau^{\mathrm{I}})}{\mathrm{d}e_m}\right|_{e_m=e_w} + \hat{S}^{\mathrm{II}}\left.\frac{\mathrm{d}(\rho_\sigma^{\mathrm{II}}\rho_\tau^{\mathrm{II}})}{\mathrm{d}e_m}\right|_{e_m=e_w}\right), \quad [18]$$

which is Eq. **3** using the same notations as in scenario 1.

Numerical simulations. We use the same linear model of vaccine escape as in scenario 1, but we allow for different vaccine efficacies depending on the number of doses:

$$\rho_\tau^{\mathrm{I}}(e_i) = 1 - r_\tau^{\mathrm{I}}(1-e_i), \quad [19]$$

$$\rho_\sigma^{\mathrm{I}}(e_i) = 1 - r_\sigma^{\mathrm{I}}(1-e_i), \quad [20]$$

$$\rho_\tau^{\mathrm{II}}(e_i) = 1 - r_\tau^{\mathrm{II}}(1-e_i), \quad [21]$$

$$\rho_\sigma^{\mathrm{II}}(e_i) = 1 - r_\sigma^{\mathrm{II}}(1-e_i), \quad [22]$$

where r_τ and r_σ give the vaccine efficacy in the absence of vaccine escape mutation (i.e., $e_i = 0$). When $e_i = 1$ (full vaccine escape), the vaccine offers no reduction in transmissibility and susceptibility ($\rho_\sigma = \rho_\tau = 1$). We assume that vaccination can also protect against disease-induced mortality, and we define r_μ^{I} and r_μ^{II} so that $\hat{\mu}_i^{\mathrm{I}} = \mu(1-r_\mu^{\mathrm{I}})$ and $\hat{\mu}_i^{\mathrm{II}} = \mu(1-r_\mu^{\mathrm{II}})$.

Initial conditions used in Fig. 2 *B–D* are as follows: $S(0) = 1$, $\hat{S}^{\mathrm{I}}(0) = \hat{S}^{\mathrm{II}}(0) = 0$, $I(0) = \hat{I}^{\mathrm{I}}(0) = \hat{I}^{\mathrm{II}}(0) = 10^{-6}$, $D(0) = 0$, and $p_m(0) = 10^{-3}$. The intensity of NPI varies with time ($c(t) = 0.7$ when $t \in [40, 140]$ and $t \in [150, 250]$, $c(t) = 0$ otherwise). Vaccination starts at $t = 150$, and the other parameters used in Fig. 2 *B–D* are listed in Table 2.

Data Availability. Mathematica notebooks have been deposited in Zenodo https://doi.org/10.5281/zenodo.5803062 (36).

Note Added in Proof. Several countries recommend a third dose of vaccination. Our scenario 2 could be readily modified to account for this new class of vaccinated individuals and this would yield a third term, $\Delta E^{\mathrm{III}}\,\hat{S}^{\mathrm{III}}$, in Eq. **3**.

ACKNOWLEDGMENTS. We thank the Editor and two anonymous reviewers for helpful and constructive comments. This work was funded by grants ANR-16-CE35-0012 "STEEP " to S.L. and ANR-17-CE35-0012 "EVOMALWILD" to S.G. from the Agence Nationale de la Recherche.

1. J. R. Goldstein, R. D. Lee, Demographic perspectives on the mortality of COVID-19 and other epidemics. *Proc. Natl. Acad. Sci. U.S.A.* **117**, 22035–22041 (2020).
2. J. R. Goldstein, T. Cassidy, K. W. Wachter, Vaccinating the oldest against COVID-19 saves both the most lives and most years of life. *Proc. Natl. Acad. Sci. U.S.A.* **118**, e2026322118 (2021).
3. K. M. Bubar *et al.*, Model-informed COVID-19 vaccine prioritization strategies by age and serostatus. *Science* **371**, 916–921 (2021).
4. J. Dushoff *et al.*, Vaccinating to protect a vulnerable subpopulation. *PLoS Med.* **4**, e174 (2007).
5. J. Dushoff, C. Colijn, D. J. D. Earn, B. M. Bolker, Transmission dynamics are crucial to COVID-19 vaccination policy. *Proc. Natl. Acad. Sci. U.S.A.* **118**, e2105878118 (2021).
6. J. Medlock, A. P. Galvani, Optimizing influenza vaccine distribution. *Science* **325**, 1705–1708 (2009).
7. L. Matrajt, J. Eaton, T. Leung, E. R. Brown, Vaccine optimization for COVID-19: Who to vaccinate first? *Sci. Adv.* **7**, eabf1374 (2021).
8. S. Bansal, B. Pourbohloul, L. A. Meyers, A comparative analysis of influenza vaccination programs. *PLoS Med.* **3**, e387 (2006).
9. M. C. Fitzpatrick, A. P. Galvani, Optimizing age-specific vaccination. *Science* **371**, 890–891 (2021).
10. S. Moore, E. M. Hill, L. Dyson, M. J. Tildesley, M. J. Keeling, Modelling optimal vaccination strategy for SARS-CoV-2 in the UK. *PLOS Comput. Biol.* **17**, e1008849 (2021).
11. J. Chen *et al.*, Prioritizing allocation of covid-19 vaccines based on social contacts increases vaccination effectiveness. medRxiv [Preprint] (2021) https://doi.org/10.1101/2021.02.04.21251012 (Accessed 6 February 2021).
12. J. R. Gog, E. M. Hill, L. Danon, R. N. Thompson, Vaccine escape in a heterogeneous population: Insights for SARS-CoV-2 from a simple model. *R. Soc. Open Sci.* **8**, 210530 (2021).
13. J. Wood, J. McCaw, N. Becker, T. Nolan, C. R. MacIntyre, Optimal dosing and dynamic distribution of vaccines in an influenza pandemic. *Am. J. Epidemiol.* **169**, 1517–1524 (2009).
14. S. Riley, J. T. Wu, G. M. Leung, Optimizing the dose of pre-pandemic influenza vaccines to reduce the infection attack rate. *PLoS Med.* **4**, e218 (2007).
15. L. Matrajt, T. Britton, M. E. Halloran, I. M. Longini Jr., One versus two doses: What is the best use of vaccine in an influenza pandemic? *Epidemics* **13**, 17–27 (2015).
16. E. M. Hill, M. J. Keeling, Comparison between one and two dose SARS-CoV-2 vaccine prioritization for a fixed number of vaccine doses. *J. R. Soc. Interface* **18**, 20210214 (2021).
17. S. Gandon, M. Mackinnon, S. Nee, A. Read, Imperfect vaccination: Some epidemiological and evolutionary consequences. *Proc. Biol. Sci.* **270**, 1129–1136 (2003).
18. P. D. Williams, T. Day, Epidemiological and evolutionary consequences of targeted vaccination. *Mol. Ecol.* **17**, 485–499 (2008).
19. S. Gandon, T. Day, The evolutionary epidemiology of vaccination. *J. R. Soc. Interface* **4**, 803–817 (2007).
20. C. M. Saad-Roy, A. B. McDermott, B. T. Grenfell, Dynamic perspectives on the search for a universal influenza vaccine. *J. Infect. Dis.* **219** (suppl. 1), S46–S56 (2019).
21. S. A. Rella, Y. A. Kulikova, E. T. Dermitzakis, F. A. Kondrashov, Rates of SARS-CoV-2 transmission and vaccination impact the fate of vaccine-resistant strains. *Sci. Rep.* **11**, 15729 (2021).
22. P. D. Taylor, Allele-frequency change in a class-structured population. *Am. Nat.* **135**, 95–106 (1990).
23. S. Gandon, Evolution of multihost parasites. *Evolution* **58**, 455–469 (2004).
24. S. Lion, Class structure, demography and selection: Reproductive-value weighting in non-equilibric polymorphic populations. *Am. Nat.* **191**, 620–637 (2018).
25. N. G. Davies *et al.*; CMMID COVID-19 Working Group; COVID-19 Genomics UK (COG-UK) Consortium, Estimated transmissibility and impact of SARS-CoV-2 lineage B.1.1.7 in England. *Science* **372**, eabg3055 (2021).
26. P. Wang *et al.*, Antibody resistance of SARS-CoV-2 variants B.1.351 and B.1.1.7. *Nature* **593**, 130–135 (2021).
27. B. Dearlove *et al.*, A SARS-CoV-2 vaccine candidate would likely match all currently circulating variants. *Proc. Natl. Acad. Sci. U.S.A.* **117**, 23652–23662 (2020).
28. J. W. Rausch, A. A. Capoferri, M. G. Katusiime, S. C. Patro, M. F. Kearney, Low genetic diversity may be an Achilles heel of SARS-CoV-2. *Proc. Natl. Acad. Sci. U.S.A.* **117**, 24614–24616 (2020).
29. C. M. Saad-Roy *et al.*, Epidemiological and evolutionary considerations of SARS-CoV-2 vaccine dosing regimes. *Science* **372**, 363–370 (2021).
30. N. Rochman, Y. Wolf, E. V Koonin, Substantial impact of post-vaccination contacts on cumulative infections during viral epidemics. *F1000 Res.* **10**, 315 (2021).
31. S. Bonhoeffer, M. Lipsitch, B. R. Levin, Evaluating treatment protocols to prevent antibiotic resistance. *Proc. Natl. Acad. Sci. U.S.A.* **94**, 12106–12111 (1997).
32. A. F. Read, T. Day, S. Huijben, The evolution of drug resistance and the curious orthodoxy of aggressive chemotherapy. *Proc. Natl. Acad. Sci. U.S.A.* **108** (suppl. 2), 10871–10877 (2011).
33. D. V. McLeod, S. Gandon, Understanding the evolution of multiple drug resistance in structured populations. *eLife* **10**, e65645 (2021).
34. M. Makhoul *et al.*, Epidemiological impact of SARS-CoV-2 vaccination: Mathematical modeling analyses. *Vaccines (Basel)* **8**, 668 (2020).
35. S. Lion, S. Gandon, Life-history evolution of class-structured populations in fluctuating environments. bioRxiv [Preprint] (2021). https://doi.org/10.1101/2021.03.12.435065 (Accessed 12 March 2021).
36. S. Gandon, S. Lion, Code for "Targeted vaccination and the speed of SARS-CoV-2 adaptation". Zenodo. https://doi.org/10.5281/zenodo.5803062. Deposited 24 December 2021.

Downloaded from https://www.pnas.org by 194.57.116.220 on June 19, 2026 from IP address 194.57.116.220.